

Long range surface plasmon resonance sensor based on side polished fiber with the buffer layer of magnesium fluoride

Xinjie Feng^{1,2} · Mei Yang^{1,2} · Yunhan Luo^{1,2} ·
Jieyuan Tang^{1,2} · Heyuan Guan^{1,2} · Junbin Fang^{1,2} ·
Huihui Lu^{1,2} · Jianhui Yu^{1,2} · Jun Zhang^{1,2} · Zhe Chen^{1,2}

Received: 30 August 2016 / Accepted: 20 February 2017 / Published online: 17 March 2017
© Springer Science+Business Media New York 2017

Abstract In this paper, a theoretical analysis of figure of merit (FOM) of a surface plasmon resonance (SPR) sensor with a buffer layer of magnesium fluoride has been carried out. While the FOM is the ratio of sensitivity and full width at half maximum and it is the measurement index for the SPR performance. The numerical simulation is based on side polished single mode fiber SPR sensor with the 66.5 μm residual fiber thickness and Drude model of metal with the 50 nm gold film thickness. Meanwhile, the comparisons for traditional surface plasmon resonance sensor, symmetrical surface plasmon resonance sensor and long range surface plasmon resonance sensor have performed differently for the FOM. The effect of sensitivity, full width at half maximum and transmittance depth has also been studied. All these studies, lead to a significant analysis to achieve the best possible design of a fiber optic SPR sensor with maximum FOM while the thickness of buffer layer is 100 nm. This design is expected to play an important role on chemical sensing and biological sensing.

Keywords Surface plasmon resonance · Side polished fiber

This article is part of the Topical Collection on Numerical Simulation of Optoelectronic Devices 2016.

Guest edited by Yuh-Renn Wu, Weida Hu, Slawomir Sujecki, Silvano Donati, Matthias Auf der Maur and Mohamed Swillam.

✉ Xinjie Feng
sonijatracy@qq.com

¹ Department of Optoelectronic Engineering, Jinan University, Guangzhou 510632, China

² Guangdong Province University Key Lab of Numerical Controlled Technology, Guangdong Polytechnic Normal University, Guangzhou 510635, China

1 Introduction

Surface plasmon resonance (SPR) sensing technology was developed in the 1970s. Since the last few decades, SPR has become a great conceptual tool for chemical and biological sensing. It has been widely used in drug screening, gene sequencing, and case detection and so on (Chegel et al. 1998; Leidberg et al. 1983; Homola et al. 1999). The resonance appears in the form of a sharp dip of output optical signal either with incident angle (angular interrogation) or wavelength (spectral interrogation). While lights travel from optically denser medium to optically thinner medium, the total reflection will take place, meanwhile, the evanescent wave will be formed and travel through the optically thinner medium. Surface plasmon wave (SPW) is a transverse magnetically (TM) polarized waves that travels along the interface and it is coupled with an evanescent wave of the same propagation constant so that strong absorption of light takes place. Due to this absorption, the output signal demonstrates a sharp dip, leading to the surface plasmon resonance. This resonance utilizes to measure the ambient refractive index (RI) (Cao et al. 2006). Among several SPR sensing structures the Kretschmann configuration in which the metallic layer is deposited directly on the base of a prism (Kretschmann and Raether 1968; Kretschmann 1971; Otto 1968) is the most popular. However, the traditional Kretschmann configuration SPR sensor has a bad stability and it cannot realize the signal online transmission. The SPR sensor based on side polished fiber structure in which the metallic layer is deposited directly on the base of a side polished fiber is the improvement of traditional Kretschmann configuration SPR sensor. It has significant advantages such as smaller size, longer transmission distance over those SPR sensors based on other structures (Leidberg et al. 1983). In this paper, a conventional SPR (CSPR) sensor is the structure with monolayer of metal film deposited directly on the waveguide layer. Sarid (1981) proposed a structure consists of a thin metal layer surrounded by two dielectric layers which have similar refractive indices. With the similarity of dielectric constant between the metal, the SPWs will travel as the standing wave. It can be well predicted that this structure has higher sensitivity, higher resolution and deeper penetration depth when compared with the conventional SPR sensor. This structure is called long range surface plasmon resonance (LRSPR) sensor. The magnesium fluoride (MgF₂) can be used as a buffer layer when designing a LRSPR sensor. Fluorine is singly charged thus makes MgF₂ has a relatively low refractive index. Its refractive index is similar with the analytic surrounding medium on the sensing area (Homola 2008). In this paper, performance of LRSPR sensor based on side polished fiber with a buffer layer of MgF₂ has been studied. The comparison of CSPR, LRSPR and symmetrical LRSPR sensor has also been studied, thus will provide a optimal design based on side polished fiber in SPR sensing area.

2 Simulation studies

2.1 Background

The scheme model and physical model of conventional SPR sensor based on side polished fiber are showed in Fig. 1. A conventional structure is consists of side polished fiber, monolayer gold film and sensing layer. A finite element method software-COMSOL has been used in the studies. The gold film is deposited directly on the base of a side polished fiber. The diameters of the core and the cladding are 8 and 125 μm , respectively. In the

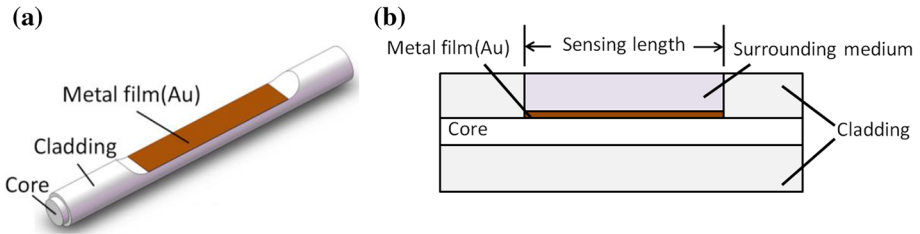


Fig. 1 a Scheme and b physical model of the side polished fiber based SPR

past work, the effect of fiber residual thickness on performance of SPR sensor has been studied. It is showed that the thicker the residual thickness is, the better the performance is (Xinjie et al. 2015). To keep the core intact, the 66.5 μm residual fiber thickness is chosen.

The refractive indices of the fiber core and fiber cladding are given as 1.4457 and 1.4378, respectively. The effect of gold film thickness on performance of SPR sensor has been studied. The thicknesses of the gold film (d_{Au}) were given 30, 40, 50, 60, 70 nm, respectively. For the dispersion in the metal layer, the Drude model (Sharma 2007) was used and given as

$$\epsilon_m = 1 - \frac{\lambda^2 \lambda_c}{\lambda_p^2 (\lambda_c + j\lambda)} \tag{1}$$

λ_p and λ_c are 168.26 and 893.42 nm, respectively. Then the square root of (1) would be took and it is given as:

$$n_m + jk_m = \sqrt{\epsilon_m} \tag{2}$$

n_m and k_m represent the real part and imaginary part of the metal refractive index. The transmittance can be given as:

$$T = \exp\left(-\frac{4\pi}{\lambda_0} \text{Im}(n_{eff})L\right) \tag{3}$$

λ_0 , n_{eff} and L represent the incidence wavelength, the effective refractive index of the metal and sensing layer length respectively. L is given 1 mm as the constant. The refractive indices of the surrounding medium are 1.37 and 1.38, respectively. By changing the wavelength, the transmittance of the SPR sensor can be calculated, and the spectra of these SPR sensors with different gold film thickness can be plotted. Figure 2 shows the spectra of these SPR sensors with different gold film thickness. It can be clearly observed that the resonant depth decrease with the increase of the gold film thickness. The sensitivity (S) and full width at half maximum (FWHM) are both two main factors in deciding whether the SPR sensor is good performance. It can be observed that as the gold film thickness become thicker, the resonant depth tends to be shallower. From these spectra, S can be calculated by:

$$S = \frac{\lambda_{res2} - \lambda_{res1}}{n_2 - n_1} \tag{4}$$

n_1 and n_2 represent the refractive indices of the surrounding mediums which are successively used in the SPR sensing tests. λ_{res1} and λ_{res2} represent the resonant wavelength while the refractive indices of the surrounding mediums are n_1 and n_2 respectively. The change

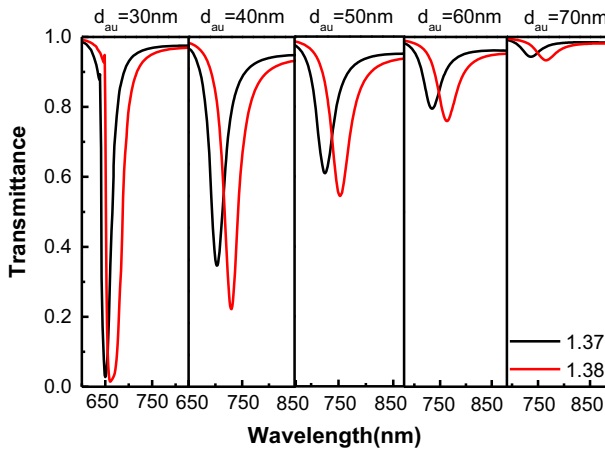


Fig. 2 The spectra of these SPR sensors with different gold film thicknesses

curves of FWHM and S with gold thickness have been plotted in Fig. 3. It can be clearly observed that the sensitivity reaches at the highest value when the thickness of the gold film is 70 nm, and the FWHM reaches at the highest value when the thickness of the gold film is 40 nm. Both of the sensitivity and the FWHM are important factors to demonstrate whether a SPR sensor has well performance. So a definition of figure of merit (FOM) of the sensor depends upon S and FWHM of the SPR curve was made and is given by:

$$FOM = \frac{S}{FWHM} \tag{5}$$

According to this relationship, the higher the S is and the lower the FWHM is, the higher the FOM is. And the larger the FOM is, the better the performance of the SPR sensor is. The histogram of FOM has been made in Fig. 4. It can be obviously observed that with the increase of thickness of gold film, FOM increase firstly and then decrease. The largest FOM appears when the gold film is 50 nm. The highest value of FOM is calculated as 82. An optimal design of conventional SPR sensor based on side polished fiber can be made

Fig. 3 The change curves of sensitivity and FWHM with different gold film thicknesses

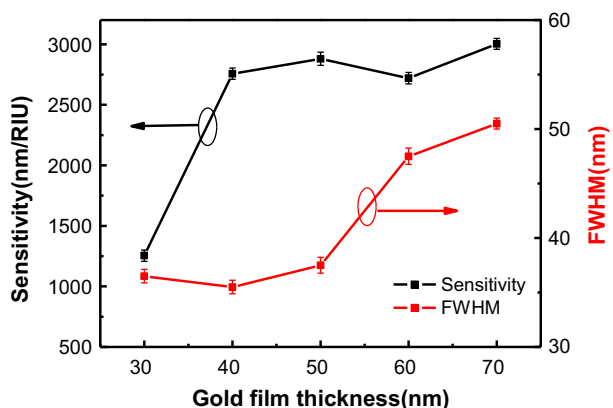
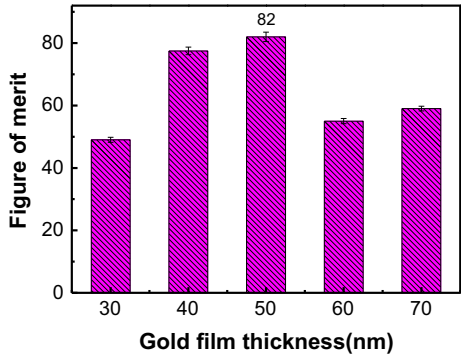


Fig. 4 The columns of FOM with different gold film thicknesses



while FOM is the largest among other situations. So the 50 nm gold film thickness has been chosen as the optimal design.

2.2 Simulation on LRSPR

A long range structure builds upon the conventional structure by adding a layer of MgF₂ as the buffer layer between the fiber and the gold film. In LRSPR sensing area, different thicknesses of buffer layer can have affect on the performance of the sensor. Thus, it is necessary to study the effect of the MgF₂ thickness on side polished fiber LRSPR sensor performance.

The physical model of LRSPR sensor based on side polished fiber with a buffer of MgF₂ has been showed in Fig. 5. The residual fiber thickness, the diameters of the core, the diameters of the cladding, the refractive index of the fiber core and the refractive index of fiber cladding are the same as Sect. 2.1. The thickness of the gold film is 50 nm. The thicknesses of MgF₂ (d_1) being used as the variable for the simulation are 0, 50, 100, 150, 300 nm respectively. Figure 6 shows the dispersion curve of MgF₂ while the wavelength ranging from 400 to 1000 nm. It is showed that MgF₂ has a refractive index in the vicinity of 1.378. To make the LRSPR perform in a better circumstance, the refractive indices of the surrounding medium are chosen as 1.37 and 1.38 respectively. The spectra of these SPR sensors with different buffer layer thickness can be plotted in Fig. 7. And the change curves of FWHM and S with gold thickness have been plotted in Fig. 8. It can be clearly observed that the sensitivity reaches at the highest value when the thickness of the MgF₂ film is 0, and the FWHM reaches at the lowest value when the thickness of the MgF₂ film is 150 m. According to the curves, the sensitivity decreases with increase of the thickness of the layer of MgF₂. When the thickness of the layer of MgF₂ is lower than 150 nm, the

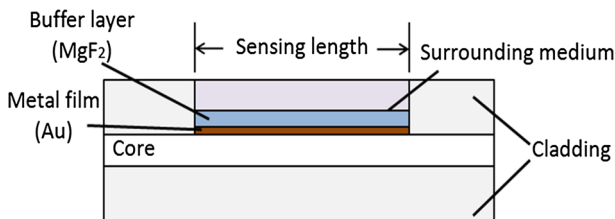


Fig. 5 The physical model of LRSPR sensor

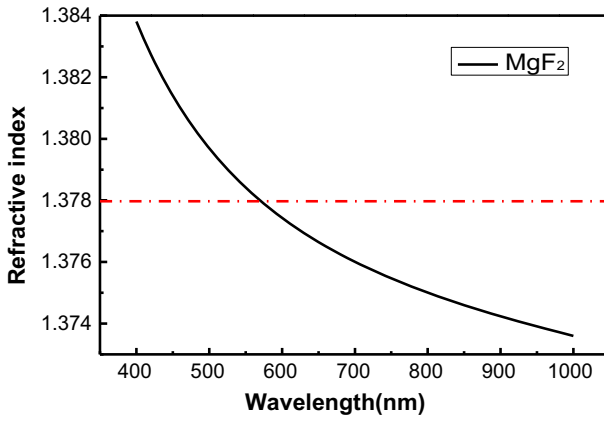


Fig. 6 The dispersion curve of MgF₂

Fig. 7 The spectra of these SPR sensors with different MgF₂ thicknesses

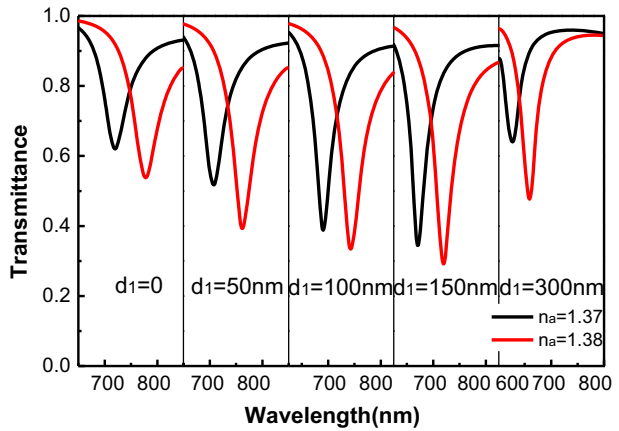
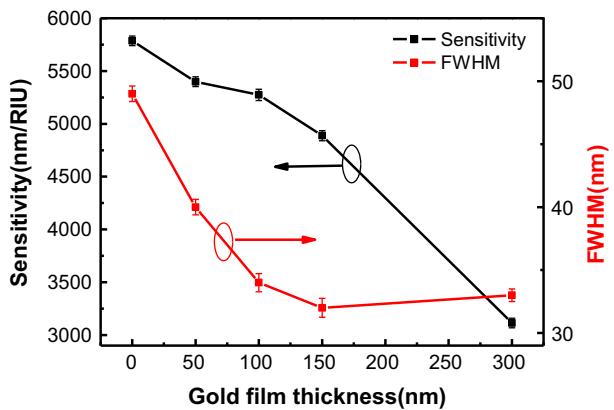


Fig. 8 The change curves of sensitivity and FWHM with different MgF₂ thicknesses

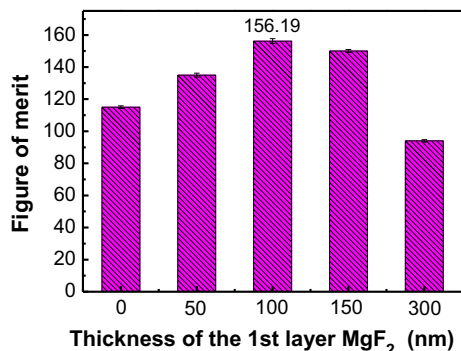


FWHM will decrease with increase of the thickness of the layer of MgF₂. A slight increment takes place when the thickness of MgF₂ layer shifts from 150 to 300 nm. The histogram of FOM has been made in Fig. 9. It can be obviously observed that with the increase of thickness of MgF₂, FOM increase firstly and then decrease. The largest FOM appears when the buffer layer is 100 nm. The maximum FOM is calculated as 156.15. An optimal design of LRSPR sensor based on side polished fiber can be made while FOM is the largest among other situations. So the 100 nm buffer layer thickness has been chosen as the optimal design.

2.3 Simulation on symmetrical SPR

A symmetrical structure builds upon the long range structure by adding a layer of MgF₂ between the gold film and the sensing layer. The physical structure based on side polished fiber with two buffers of MgF₂ has been showed in Fig. 10. The residual fiber thickness, the diameters of the core, the diameters of the cladding, the refractive index of the fiber core and the refractive index of fiber cladding are the same as Sect. 2.1. The thickness of the gold film is 50 nm. The first layer of MgF₂ is the one which is adhesive between the side polished fiber and the metal film. The second layer of MgF₂ is the one which adhesive above the metal film. The given thicknesses of first and the second layer of MgF₂ (d_1 \d d_2) are 50 nm\50 nm, 50 nm\100 nm, 100 nm\100 nm, 150 nm\150 nm, and 300 nm\300 nm respectively. The refractive indices of the surrounding medium are chosen as 1.37 and 1.38 respectively. The spectra of these SPR sensors with different buffer layer thickness can be plotted in Fig. 11. And the change curves of FWHM and S with MgF₂ thickness have been plotted in Fig. 12. It can be clearly observed that the sensitivity reaches at the highest value when the thickness of the first layer MgF₂ film is 50 nm and the thickness of the second layer MgF₂ film is 50 nm. Furthermore the FWHM reaches at the lowest value when the first layer MgF₂ film is 300 nm and the thickness of the second layer MgF₂ film is 300 nm. According to the curves, the sensitivity decreases with increase of the thicknesses of the both two layers of MgF₂, meanwhile, the FWHM decreases with increase of the thicknesses of the both two layers of MgF₂, too. The histogram of FOM has been made in Fig. 13. According to the histogram, the FOM decreases with increase of the thicknesses of the both two layers of MgF₂. It can be obviously observed that the largest FOM appears when the first layer of buffer layer is 50 nm and the second layer of buffer layer is 50 nm. The maximum FOM is calculated as 89. An optimal design of symmetrical LRSPR sensor based on side polished fiber can be made while FOM is the largest among other situations.

Fig. 9 The columns of FOM with different MgF₂ thicknesses



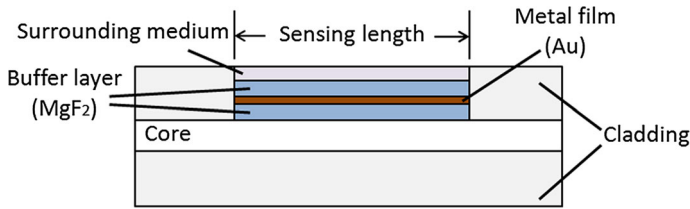


Fig. 10 The physical model of symmetrical LRSR sensor

Fig. 11 The spectra of these SPR sensors for different thicknesses of the 1st and 2nd layer of MgF₂

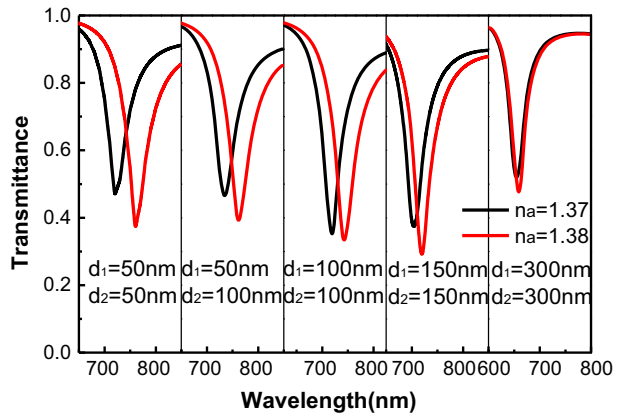
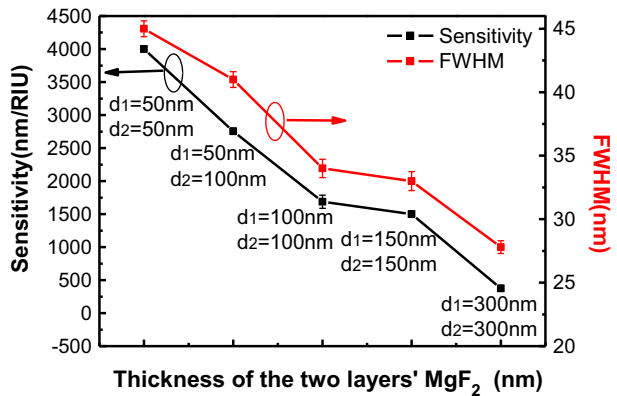


Fig. 12 The change curves of sensitivity and FWHM with different thicknesses of the 1st and 2nd layer of MgF₂



So the structure with 50 nm first buffer layer and 50 nm second buffer layer has been chosen as the optimal design.

2.4 Comparison

Table 1 shows the main parameters for the optimal design of CSPR, LRSR and symmetrical LRSR which are based on side polished fiber. The optimal design of LRSR has the largest sensitivity among those optimal designs based on CSPR structure and symmetrical SPR structure. Further, the FWHM of the LRSR is the smallest and equals to

Fig. 13 The columns of FOM with different thicknesses of the 1st and 2nd layer of MgF₂

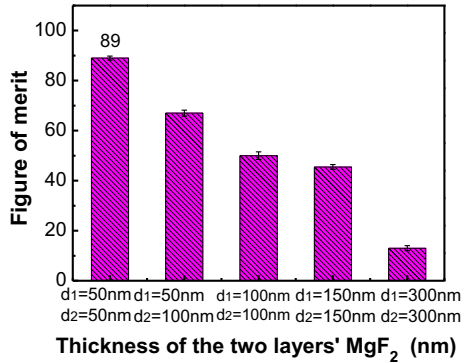


Table 1 The main parameters for the optimal design of CSPR, LRSR and symmetrical LRSR which are based on side polished fiber

Parameters	CSPR	LRSR	Symmetrical LRSR
d _{Au} (nm)	50	50	50
d ₁ (nm)	0	100	50
d ₂ (nm)	0	0	50
S (nm/RIU)	2850	5276.4	4020
FWHM (nm)	35	34	45.1
FOM (RIU ⁻¹)	82	156.19	89.1

34 nm. So the largest FOM is 156.19 while the optimal design is based on LRSR, and it is 1.9 times as the CSPR one.

Figure 14 shows the resonance spectra for CSPR, LRSR and symmetrical SPR with different surrounding medium refractive index ranging from 1.33 to 1.38 at 0.01 intervals respectively. It can be seen from the figures that there is difference in resonance wavelengths for different surrounding medium refractive index. As the surrounding medium refractive index increases, the resonant dip shifts towards longer wavelength, which indicates that, for the same structure of the SPR sensor, the resonance condition is satisfied at different wavelengths for different surrounding medium refractive index. Further, the FWHM of the LRSR is the smallest and equals to 34 nm. The plot of different wavelength with different refractive index and the sensitivity fitted curves were showed in Fig. 15. It can figure out the average sensitivity of the three types of SPR sensors by taking the average slope of these fitted curves. It can be calculated that the average sensitivity of

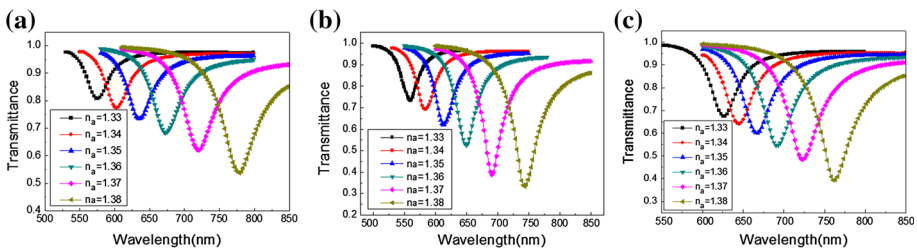


Fig. 14 a The resonance spectra for CSPR, b the resonance spectra for LRSR, c the resonance spectra for symmetrical SPR. ALL of their surrounding medium refractive index are ranging from 1.33 to 1.38

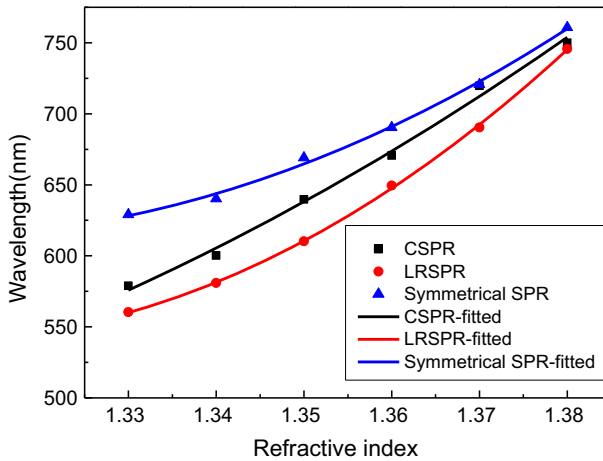


Fig. 15 The sensitivity fitted curves for the C SPR, Symmetric SPR and the LR SPR

Table 2 The FWHM, average sensitivity and FOM for the C SPR, symmetrical SPR and LR SPR

Structure	C SPR	LR SPR	Symmetrical SPR
FWHM (nm)	35	34	45.1
Average sensitivity (nm/RIU)	3558	3628	2631
FOM (RIU ⁻¹)	101.65	106.71	58.33

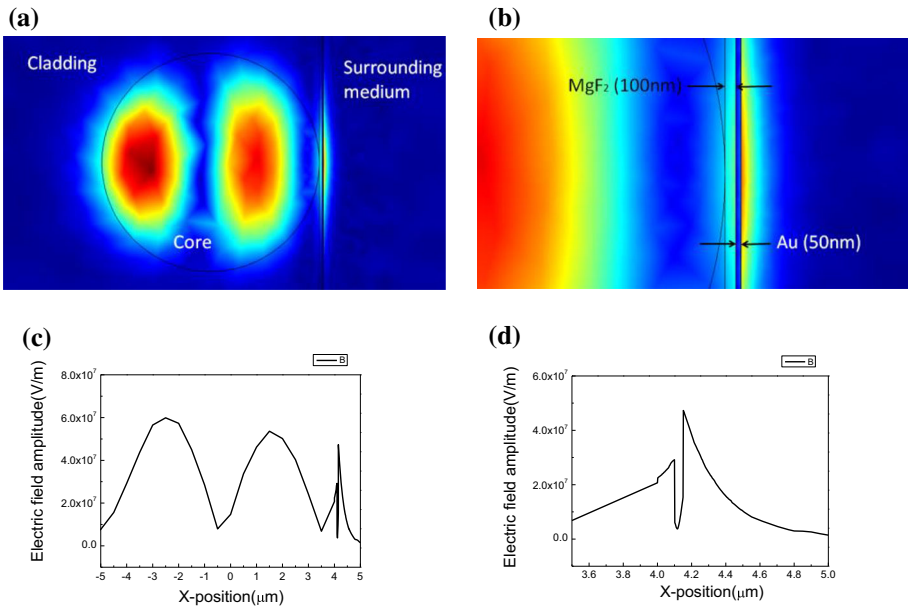


Fig. 16 The electric field distribution at the SPR resonant wavelength 690 nm while the thickness of buffer layer is 100 nm. **a, b** The total area electric field distribution and the local electric field distribution respectively. **c, d** The cross-section plot of the total electric field in Fig. 16a and the cross-section plot of the local electric field in Fig. 16b respectively

the LRSPR is the largest and equals to 3628 nm/RIU. Table 2 shows the FWHM, average sensitivity and FOM for the CSPR, Symmetrical SPR and LRSPR sensors. The maximum FOM of all these sensors is 106.71 for the structure of LRSPR. The minimum FOM of all these sensors is 58.33 for the structure of symmetrical SPR. It can be observed that in this situation which the surrounding medium refractive index ranging from 1.33 to 1.38, the performance of LRSPR sensor still perform better than CSPR sensor and symmetrical SPR sensor. It can be observed that LRSPR structure has higher sensitivity, narrower FWHM and larger FOM than other two structure of SPR sensor. Figure 16a shows the electric field distribution at the SPR resonant wavelength 650 nm while the thickness of buffer layer is 100 nm. Figure 16b shows the local area which is near the buffer layer and the metal film of Fig. 16a. Figure 16c, d shows the cross-section plot of the total electric field in Fig. 16a and the local total electric field along the direction perpendicular to the fiber base in Fig. 16b respectively. From these figures showed in Fig. 16, it can be observed that there are both clear electric field amplitude enhancement in each side of the metal film. The enhancement which takes place above the interface between the metal film and the surrounding medium tends to be larger than the enhancement which takes place above the interface between the metal film and buffer layer.

3 Conclusion

The FOM is a key factor to measure the performance of the SPR sensors because it provides higher sensitivity and thinner FWHM. The FOM is used as the measurement indicator in these studies about providing the optimal designs which are based on conventional SPR, LRSPR and symmetrical SPR structure respectively. The optimal design of conventional SPR sensor based on side polished fiber has the 50 nm gold film thickness. The optimal design of LRSPR sensor based on side polished fiber can has the 100 nm buffer layer thickness has been chosen as the optimal design. The optimal design of symmetrical SPR sensor based on side polished fiber has the 50 nm first buffer layer and 50 nm second buffer layer.

The comparisons have been made to discuss the differences of the sensitivity, FWHM and FOM among all these optimal design based on conventional SPR, LRSPR and symmetrical SPR structures. All these studies lead to a significant analysis to achieve the best possible design of a fiber optic SPR sensor with the maximum FOM while the thickness of buffer layer with MgF₂ is 100 nm based on side polished fiber LRSPR structure. This design is well expected to be applied in the SPR sensor field and will play an important role in the field of optical fiber biosensor and chemical sensing.

Acknowledgements This work is supported by the National Natural Science Foundation of China (Nos. 61177075, 61008057 and 61275046), the State Key Laboratory of Precision Measuring Technology and Instruments (No. PIL1406) and the Fundamental Research Funds for the Central Universities of China (No. 21614313).

References

- Cao, Z.X., Wu, L.N., Li, D.: Distributed optical fiber surface plasmon resonance sensors. *Chin. Opt. Lett.* **4**, 160–163 (2006)
- Chegel, V.I., et al.: Surface plasmon resonance sensor for pesticide detection. *Sens. Actuators B* **48**, 456–460 (1998)

- Homola, J.: Surface plasmon resonance sensors for detection of chemical and biological species. *Chem. Rev.* **108**(2), 462–493 (2008)
- Homola, J., Sinclair, S., Gauglitz, G.Y.: Surface plasmon resonance sensors: review. *Sens. Actuators B* **54**, 3–15 (1999)
- Kretschmann, E.: Die Bestimmung optischer Konstanten von Metallen durch Anregung von Oberflächenplasmaschwingungen. *Z. Phys.* **241**, 313–324 (1971)
- Kretschmann, E., Raether, H.: Radiative decay of non radiative surface plasmons excited by light. *Z. Naturfr.* **23**, 2135–2136 (1968)
- Leidberg, B., Nylander, C., Sundstrom, I.: Surface plasmon resonance for gas detection and biosensing. *Sens. Actuators* **4**, 299–304 (1983)
- Otto, A.: Excitation of nonradiative surface plasma waves in silver by the method of frustrated total reflection. *Z. Phys.* **216**, 398–410 (1968)
- Sarid, D.: Long-range surface-plasma waves on very thin metal films. *Phys. Lett.* **47**(26), 1972–1980 (1981)
- Sharma, A.K.: On the performance of different bimetallic combinations in surface plasmon resonance based fiber optic sensors. *J. Appl. Phys.* **101**, 09311 (2007)
- Xinjie, F., Peiling, M., Xiaolong, C.: Design and optimization of surface plasmon resonance sensor based on side polished single-mode fiber. *Spectrosc. Spectr. Anal.* **35**(05), 1419–1423 (2015)